Study of spin-wave-turbulence attractor geometry in antiferromagnetic CsMnF₃

A. I. Smirnov

Institute of Physical Problems, Academy of Sciences of the USSR

We study the geometry of attractors for various regimes of spin-wave turbulence in CsMnF₃. In this experiment turbulence consists of temporally irregular sequences of bunching and rarefaction of magnons which are excited parametrically by microwave pumping. In the case of chaotic regimes which occur through the development of a period-doubling cascade (according to the Feigenbaum scenario), the attractors have a two-dimensional local structure with folding and branching and with subsequent layering. A feature of this class of chaotic regimes is that the complication of the motion is accompanied by a complication of the topological structure of the attractor, while its embedding dimensionality is conserved. We obtain exact topological attractor structures. For chaotic regimes in the region of strong magnetic fields which occur in the Pomeau-Manneville scenario the attractors have a dimensionality which changes from 3 to 5 when chaos sets in.

1. INTRODUCTION

Experiments with parametric excitation of a rather large number of magnons in antiferromagnetic CsMnF₃ have revealed[1] a particular form of turbulence–a redistribution, which is irregular in time, of the magnon density in the sample. The transition from the regime of a uniform stationary magnon distribution in the sample volume to turbulence takes place via a periodic regime of bunching and rarefaction cycles, and after that according to a Feigenbaum or Pomeau-Manneville scenario. A detailed study of the transitional regimes was performed in Ref. 2. We gave there a diagram of different periodicity regimes and of chaotic regimes in the pumping-power-P–magnetic-field-H plane. Apparently, the bunching occurs due to the mutual attraction of the magnons and the non-stationarity of the process in time is connected with the depletion of magnons in the strong condensation region due to the non-linear damping and the overheating of the sample.[1,2] There are two chaotic regime regions which, following Ref. 2, we call "chaos 1" and "chaos 2"; they correspond to different regions of P and H values. We described in Ref. 2 possible causes for chaotization in the transition to each of these.

According to the modern approach to the problem of the onset of turbulence, the basis of the many forms of chaotic motion in distributed systems is the change with time of only a few important variables which determine the dynamics of the system. Algorithms have been worked out which allow one directly to determine from experiments several "independent" variables which uniquely determine the potentially infinite dimensional motion of a dissipative continuous system, when the number of degrees of freedom which in actual fact is involved in the motion is not known *a priori* (we quote here Ref. 5). The number of these variables, whose values are unambiguously connected with the position of the system in its actual phase space, is called the dimensionality n_c of the embedding.[3–5] The aim of the present paper was in this connection to use the algorithms of Refs. 3–5 to establish the dimensionality of the embedding for the various regimes of spin-wave turbulence which are described in Refs. 1 and 2 and, if possible, to establish the topological structure of the attractors for those regimes.

2. CONSTRUCTION OF THE PHASE SPACE AND DIMENSIONALITY OF THE EMBEDDING

To construct a multidimensional phase portrait we use the method described in Refs. 3–5. Examples of its realization for an analysis of experimental data are given, in particular, in Refs. 5–8. According to this method one can take for the equivalent phase coordinates at time t the variables $x_i = a[t + \tau(i - 1)]$, where $a(t)$ is the only measurable quantity (one of the actual phase coordinates or a function of the position in the actual phase space), and τ is an arbitrary time shift. In order that the position in the equivalent phase space be in an unambiguous one-to-one correspondence with the position in the real phase space it is sufficient that the number of variables x_i be not less than $2n_H + 1$, where n_H is the Hausdorff dimensionality of the attractor in the real phase space.[4] In those cases where the geometry of the attractor is simple and its mapping into the space of equivalent variables has no self-intersections, the number n_c can be lowered down to n_H.

If the number of important variables is not known *a priori*, as is the case in most experiments with distributed systems, we must also determine from the experiment how many coordinates describe the evolution of the system. To do that we use a convenient geometric criterion, formulated in Ref. 5, which is equivalent to the criterion of the simultaneous probability distribution.[3] If $n > n_c$, any measurable quantity $y(t)$ must be a function of the n phase variables which we have constructed: $y(t) = f(x_1,...,x_n)$. If $n < n_c$, the variable y is in the general case not a function of $x_1,...,x_n$ and one must add it as an $n + 1$st coordinate. Starting from $n = 1$ one must thus add one coordinate by the method described above and test it on whether it is functionally independent of the previous ones. When the point $\mathbf{x}(t)$ moves the recurrence of the vector $\mathbf{x}$ does or does not lead to the recurrence of y, depending on whether or not there is a functional dependence.

It is convenient to check this fact graphically. To do this in a graph we plot along the abscissa the distance

$$r_n = \left\{ \sum_i^n [x_i(t) - x_i^0]^2 \right\}^{1/2}$$

from the moving position of a point on the attractor to some point x^0 fixed on it, and along the ordinate axis the quantity

$$d = |x_{n+1}(t) - x_{n+1}^0|.$$

If there is a functional dependence as described above, $d \to 0$, as $r_n \to 0$. We call this manner of checking a functional dependence "criterion 1." To realize it there need be only a few points on the attractor in a n-dimensional sphere with a small radius, in contrast to the methods determining the Hausdorff dimensionality of the attractor. The authors of Ref. 5 have made the above described criterion even coarser by completely eliminating from it all small scales. According to the coarsened criterion the dimensionality n_c is attained if the envelope trajectory in the r_n, d plane lies completely below the line $d = k r_n$, where $k \approx 1$. We call this criterion "criterion 2"; it can be very useful to estimate large embedding dimensionalities when the number of experimental points on an attractor in the volume bounded by small linear dimensions is small. The dimensionality n_c obtained by the criteria 1 and 2 can in some actual cases be lowered, for instance, using the procedure of additional sections, as is described below, or by using a rotated system of coordinates.

3. EXPERIMENTAL RESULTS AND THEIR PROCESSING

As the above-mentioned measurable quantity $a(t)$ we shall use the microwave power passing through a cavity with a sample (see the experimental setup in Ref. 2). The value of the transmitted power is determined by its absorption in the sample and also by the value of the real part of the high-frequency susceptibility, and depends thus on the number of magnons, their damping, and other quantities changed by the spin-wave turbulence process. The experiment was carried out on the same CsMnF$_3$ sample and under the same experimental conditions as those described in Ref. 2: the frequency of the microwave source was 18 GHz, the temperature 1.4 K, and so on. We studied the geometry of the attractors for five chaotic regimes; the oscillograms of the microwave signal for those regimes are shown in Fig. 1, where we also show the oscillogram for the periodic redistribution regime. The oscillograms were recorded in numerical form in the computer memory. For each of the regimes the record in the computer memory is 10 sections of 1024
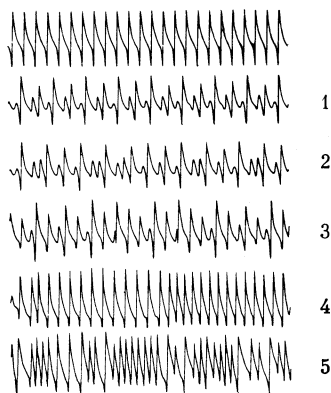
FIG. 1. Filtered oscillograms of microwave power passing through a cavity. The upper oscillogram is the periodic regime, 1–5 are chaotic regimes. The scanning time is 2 ms for the oscillograms 1–3 and the periodic regime, and 5 ms for the oscillograms 4 and 5.

values separated by time intervals $t_d = T/1024$, where T is the scanning time of each section. We show in Fig. 1 one section for each of the regimes, i.e., one tenth of the experimental data used to construct and to study the attractors. To suppress the noise of the receiver-amplifier circuit we subjected the function $a(t)$ to a numerical Fourier filter cutting off the spectral components with frequencies exceeding $20 f_0$, where f_0 is the average frequency of the sequence of bunching-rarefaction processes. Such a filter not only suppresses the noise, but also smoothes somewhat the peaks of the oscillogram. The amplitude of the spikes of the microwave signal is decreased by about 20% in the filtering, but the part of the oscillogram which is the main one in duration is not distorted. The use of unfiltered functions $a(t)$ gives the same values of n_c for the regimes 1–4 in Fig. 1 as the unfiltered signal, but the elements of the fractal structure of the attractors are not resolved. For regime 5 the embedding dimensionality is not reached up to $n = 8$ when we use the unfiltered signal. The phase portraits in the x_1, x_2 plane are given in Fig. 2.

The regimes 1–3 of the present paper correspond to chaos 1 in the diagrams of Fig. 3 of Ref. 2 and the regimes 5, 8, 11 in Fig. 5 in Ref. 2. The regimes 4 and 5 of the present paper correspond to chaos 2 in the regime diagram and correspond approximately to the regimes 3 and 5 in Fig. 4 of Ref. 2. The regime 4 is transitional from the main period cycle to chaos 2.

The construction of the trajectories in the r_n, d plane gives, according to criterion 1, the following embedding dimensionalities: for the regimes 1–3, $n_c = 3$, for regime 4, $n_c = 3$, for regime 5, $n_c = 5$ according to criterion 1 and $n_c = 6$ according to criterion 2. The realization of the algorithm to determine n_c is illustrated for regime 5 in Fig. 3. To determine n_c for each of the regimes the construction procedure in the r_n, d plane was carried out for not less than 20 points x^0 located at different positions of the attractor and for different values of τ in the interval (2 to 10) t_d.

The attractors embedded in three-dimensional space allow a more detailed study of their form when planar sections are passed. We show in Fig. 4 a number of sections of the attractor corresponding to the regime 2. We see that the points in which the phase trajectory crosses the intersecting plane are positioned on line segments, i.e., the attractor is made up of a two-dimensional strip which forms line segments when it crosses the intersecting planes. These plane strips from folds and also branches in the plane of the strip with a subsequent layering of the branch part on the main part. The process of the formation of a fold can be traced when we go from section 4 to section 3. The lower points of the right-hand branch of section 4 goes over into the lower part of the left-hand branch of the section 3.

The construction of a large number of sections enables us to obtain unambiguously the topological structure of the attractor for each of the regimes 1–3. The topological equivalents of these attractors are drawn in Fig. 5.

For the regime 1 the attractor is topologically equivalent to the Rössler attractor (see, e.g., Ref. 9) for the regime of motion in two chaotic zones—a two-loop spiral formed from a plane strip with folds. When the Rössler attractor evolves in the direction of increasing the region of chaotic change of the variables, the folds are embedded into one another, as a result of which one loop is formed from a plane strip with a fold. The chaotization of the motion is then due
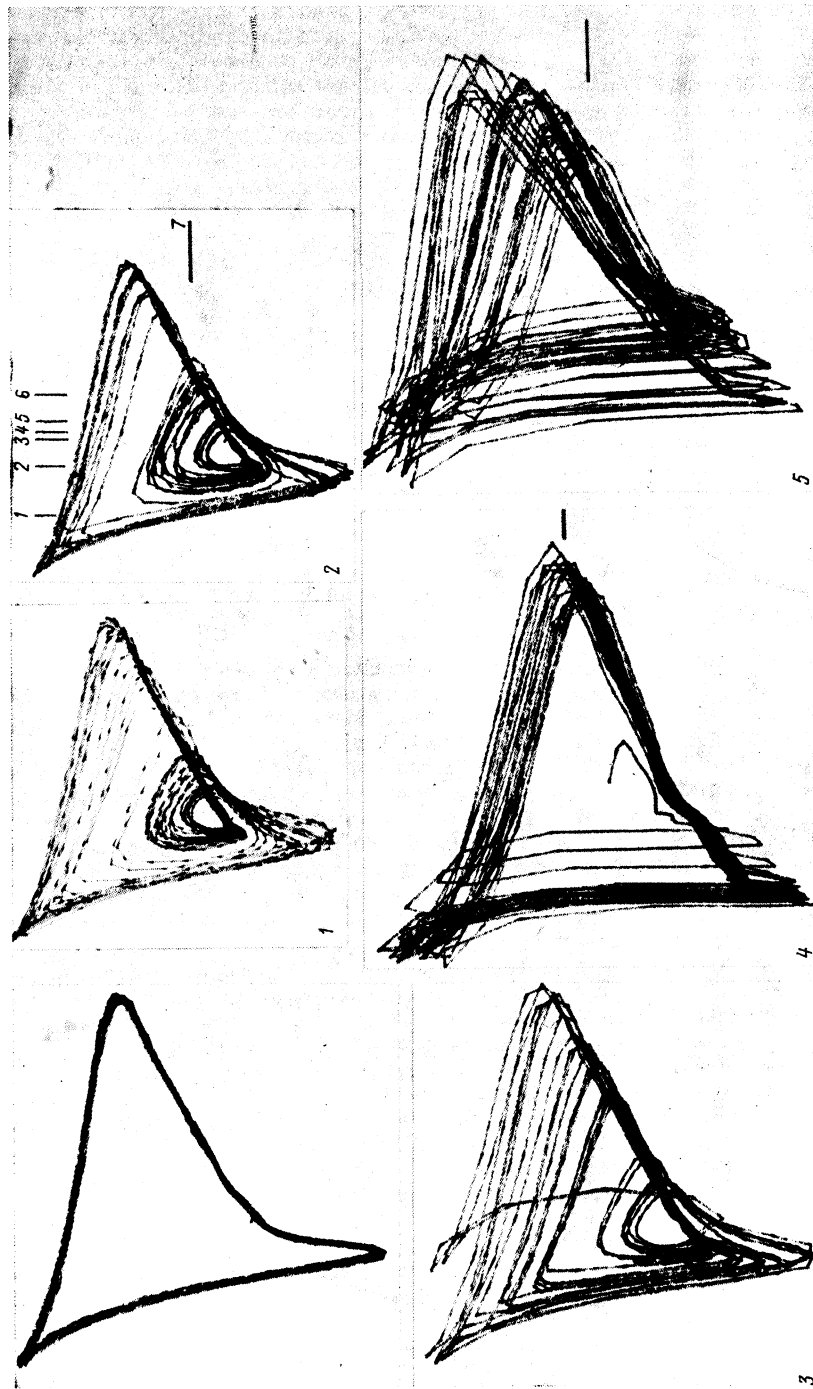
FIG. 2. Phase portraits for the periodic and chaotic regimes, $\tau = 5t_d$. For the regimes 2, 4, and 5 we have indicated the directions of the sections given, respectively, in Figs. 4 and 6.
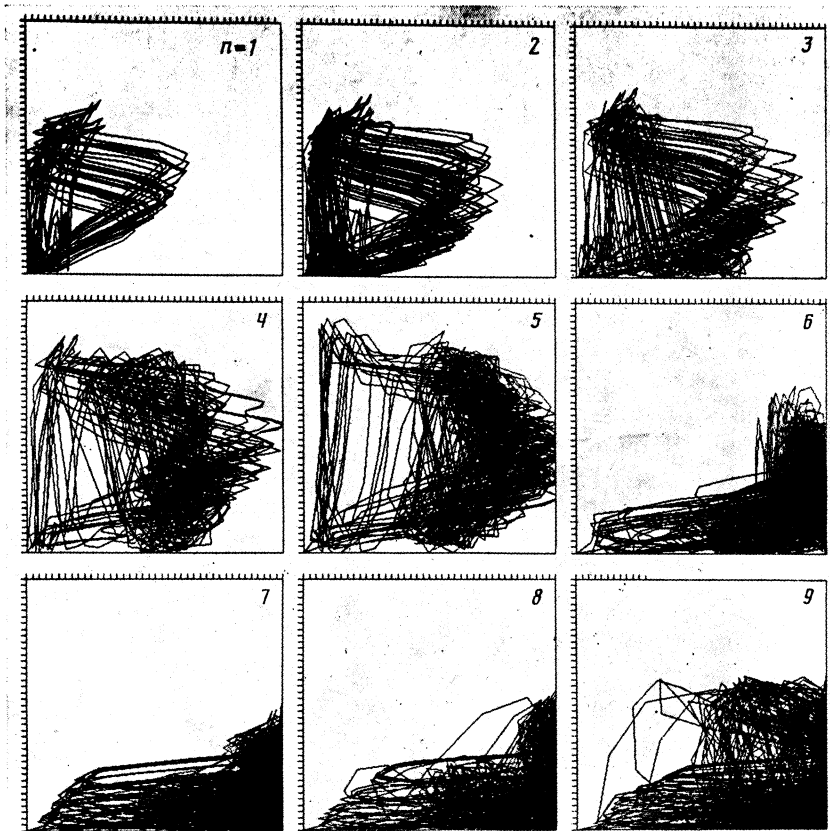
FIG. 3. Scanning of the functional dependence of the $n + 1$st coordinate on the preceding ones for the regime 5; $\tau = 5t_d$, $n = 1$ to 9.

to the divergence of the trajectories in the plane of the strip and their mixing as the result of the embedding (the so-called stretching and embedding).

The development of the attractor of spin-wave turbulence proceeds differently. When we go over to regime 2 a small plane band is branched off in the plane of the strip, departs from the large loop, and is superposed on the trajectory of the small loop when their planes gradually converge. Such a chaotization of the trajectories occurs in the Lorenz attractor.[9] In the attractor of regime 3 there occurs a fusion
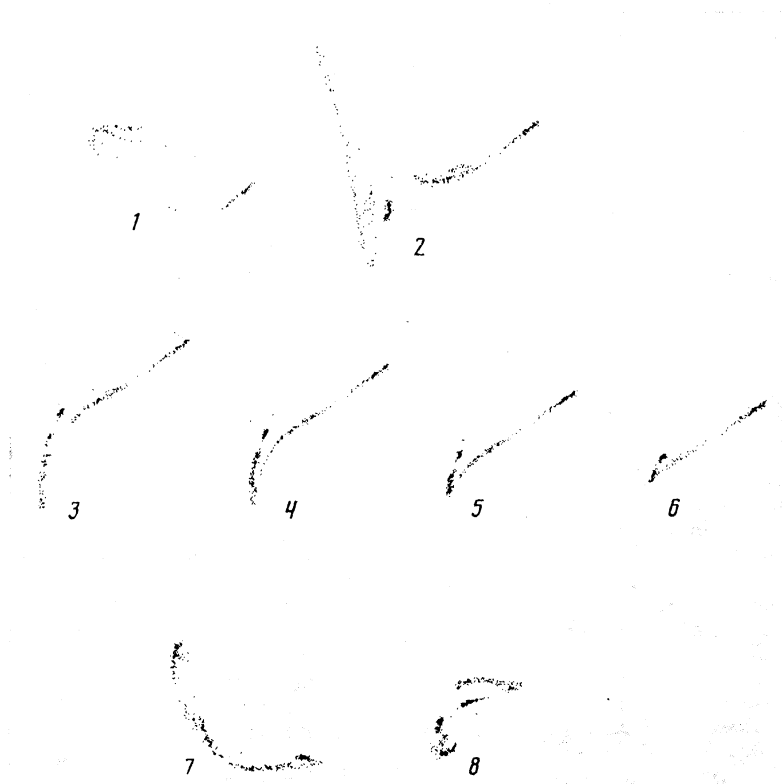
FIG. 4. Sections of the attractor for the regime 2. The plane of the section 8 is parallel to the plane of Fig. 2.
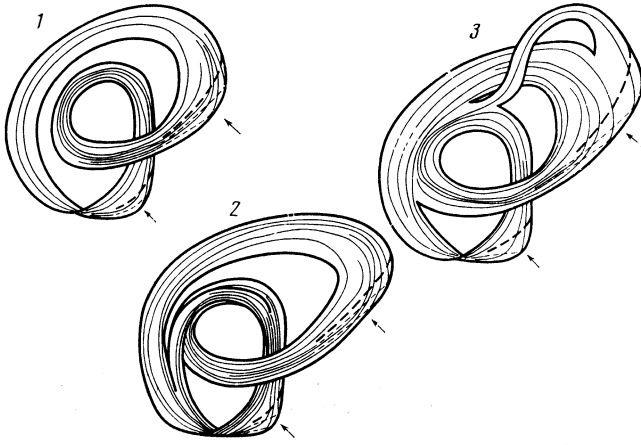
FIG. 5. Topological equivalents of the attractors for the regimes Nos 1–3. The arrows indicate the folds.

of the edges of the strip at the large and small loops, and the band which branches off like a Lorenz attractor moves over from the interior to the exterior orbits, forming there one more fold.

The attractors for the regimes corresponding to chaos 1 can thus be constructed from elements of Rössler and Lorenz attractors. They correspond to motion with the smallest chaotization in the sense that the phase trajectories in them diverge in only one direction (they possess only one positive Lyapunov exponent). Possible types of attractors for different flow dimensionalities, i.e., orders of the system of differential equations determining the evolution of the dynamical system, are enumerated, e.g., in Ref. 10. We note that for three-dimensional flows only one more kind of locally two-dimensional attractors are possible apart from the ones described above—a torus, but it differs from a strange attractor with exponential divergence of trajectories because there is no continuous Fourier spectrum for the functions $x_i(t)$.

The sections described here demonstrate also the features of the fractal structure of the attractor—a layer, which with some finite accuracy can be assumed to be two-dimensional, is shown to contain additional layer when the scale of resolution is decreased, and these, in turn, also must consist of layers, and so on. For example, one sees in the section 5 the layered structure of an attractor strip which gives a section branch inclined to the vertical axis of the figure at an angle of approximately 45°.

The sections for the regimes 4 and 5 demonstrate the
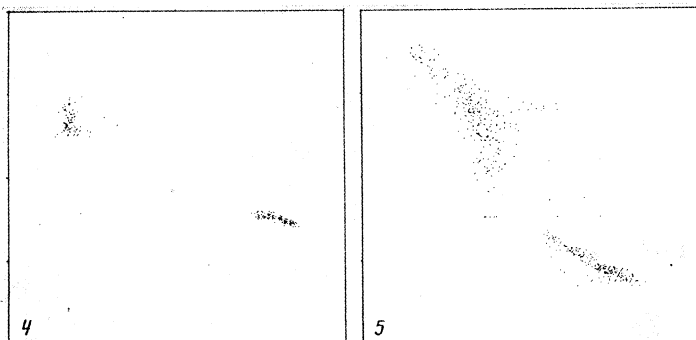
three-dimensional nature of the projections of the corresponding attractors in three-dimensional space—the points where the trajectories intersect the section planes fill two-dimensional sectors. The mixing of the trajectories in the regime 4 thus occurs in a three-dimensional tube of trajectories (the divergence occurs in two directions and the flow dimensionality is not less than 4), while for the regime 5 the trajectories mix in a space of yet more dimensions, but its dimensionality is bounded and is not larger than 5.

4. DETERMINATION OF THE SCALING DIMENSIONALITIES

Nowadays several forms of scaling dimensionalities are defined for attractors.[10] Such a dimensionality is defined as the exponent of the function $C \propto l^d$, where C is a quantity connected with the small linear dimension l of a region on the attractor. Of greater interest is the Hausdorff definition of dimensionality, n_H, as that quantity indicates not only the fact that the dimensionality of the process is finite, but also the fractal nature of the attractor. However, to determine n_H from experiment it is necessary that the number of experimental points in a small region of the attractor be of the order of 10^{n_H},[5,11] and so far this has been impossible to realize for $n_H \gtrsim 4$. The authors of Ref. 11 proposed to define a so-called correlation dimensionality ν for which they chose as C the average number of points falling in a sphere of radius l:

$$C(l) = \lim_{N \to \infty} \frac{1}{N^2} \sum_{i,j=1}^{N} H(l - r_{ij}^n), \qquad (1)$$

where N is the number of points on the attractor over which we sum, H the Heaviside function, and r_{ij}^n the distance between points in the n-dimensional space. As we are summing over a large number of points, the demands on the density of points are here not so critical. The dimensionality ν is the same as n_H for a uniform distribution of points along the attractor, and in the general case bounds n_H from below.[11] For spin-wave turbulence the points are not distributed uniformly as there is a part of the attractor along which the motion along the trajectories proceeds fast, and a part along which the majority of points is situated, where the motion is slow. In our case, the determination of ν gives thus information about the finite dimensionality of the attractor and bounds n_H from below. We carried out the determination of ν similarly to Ref. 12 for 25 different i in (1) and 3 different values of τ. We give the dependence of $\ln C$ on $\ln l$ for regime 5 in Fig. 7. From the slope of these curves for large dimensionalities n of the reconstructed phase space we determine $\nu = 3.2 \pm 0.3$. For regime 4, $\nu = 2.2 \pm 0.2$, and for regime 2, $\nu = 2.0 \pm 0.2$.

FIG. 6. Sections of the attractors for the regimes 4 and 5.
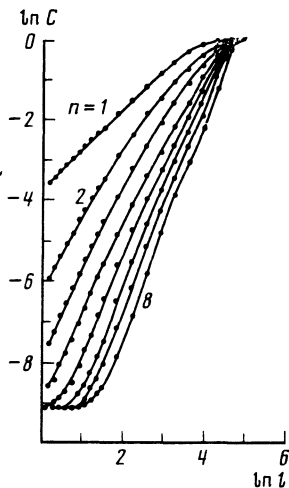
FIG. 7. Determination of the correlation dimensionality ν for the regime 5.

5. CONCLUSION

summarizing the present study we note a few aspects which distinguish spin-wave turbulence from other phenomena that exhibit a behavior typical of dynamic chaos (see, e.g., Refs. 5–7). In the region of the parameters P and H, in which the chaotic regimes develop through a period-doubling cascade, the complication of the regime (i.e., the increase in the amplitude of the chaotic component of the density oscillations) occurs for a constant number of degrees of freedom involved in the motion and is accompanied by a complication of the topological structure of the attractor. The topological structure differs by having an unusual combination of elements of the Rössler and Lorenz attractors which are characteristic of the simple model-equation systems.

In the case of hydrodynamic turbulence, which has

been studied before,[5,6] the complication of the regime occurs through an increase in the number of degrees of freedom involved in the motion, while in chemical turbulence[7] the complication takes place in the framework of a Rössler-type attractor with a simplified topological structure.

There is also a region of the above-mentioned parameters in which the number of effective degrees of freedom increases when we change to developed turbulence—for chaos 2 the embedding dimensionality of the attractor increases, starting from 3, but for advanced turbulence it remains not larger than 5.

[1] A. I. Smirnov, Zh. Eksp. Teor. Fiz. 88, 1369 (1985) [Sov. Phys. JETP 61, 815 (1985)].
[2] A. I. Smirnov, Zh. Eksp. Teor. Fiz. 90, 385 (1986) [Sov. Phys. JETP 63, 222 (1986)].
[3] N. H. Packard, J. P. Crutchfield, J. D. Farmer, and R. S. Shaw, Phys. Rev. Lett. 45, 712 (1980).
[4] F. Takens, Lecture Notes in Mathematics 898, 366 (1981).
[5] S. N. Lukashchuk, A. A. Predtechenkiĭ, G. E. Fal'kovich, and A. I. Chernykh, (The calculation of attractor dimensionality from experimental data, Preprint 280, Institute of Automation and Electrometry, Siberian Division, Acad. Sc. USSR, Novosibirsk, 1985.
[6] A. Brandstätter, J. Swift, H. L. Swinney et al., Phys. Rev. Lett. 51, 1442 (1983).
[7] J.-C. Roux, R. H. Simoyi, and H. L. Swinney, Physica D8, 257 (1983).
[8] H. Yamazaki, M. Mino, H. Nagashima, and M. Warden, J. Phys. Soc. Japan 56, 742 (1987).
[9] A. J. Lichtenberg and M. A. Lieberman, Regular and Stochastic Motion, Springer, Berlin, 1983, Ch. 7.
[10] A. Wolf, J. B. Swift, H. J. Swinney, and J. A. Vastano, Physica D16, 285 (1985).
[11] P. Grassberger and I. Procaccia, Physica D9, 189 (1983).
[12] B. Malraison, P. Atten. P. Berge, and M. Dubois, J. de Phys. Lett. 44, L-897 (1983).

Translated by D. ter Haar